

Supplementary Information for "21st century response of Petermann Glacier, northwest Greenland to ice shelf loss"

Emily A. HILL,^{1*} G. Hilmar GUDMUNDSSON,² J. Rachel CARR,¹ Chris R. STOKES³ Helen M. KING²

CONTENTS

1. Text S1
2. Figures S1 to S6

*Present address: Department of Geography and Environmental Sciences, Northumbria University, Newcastle-upon-Tyne, NE1 8ST, UK UK.

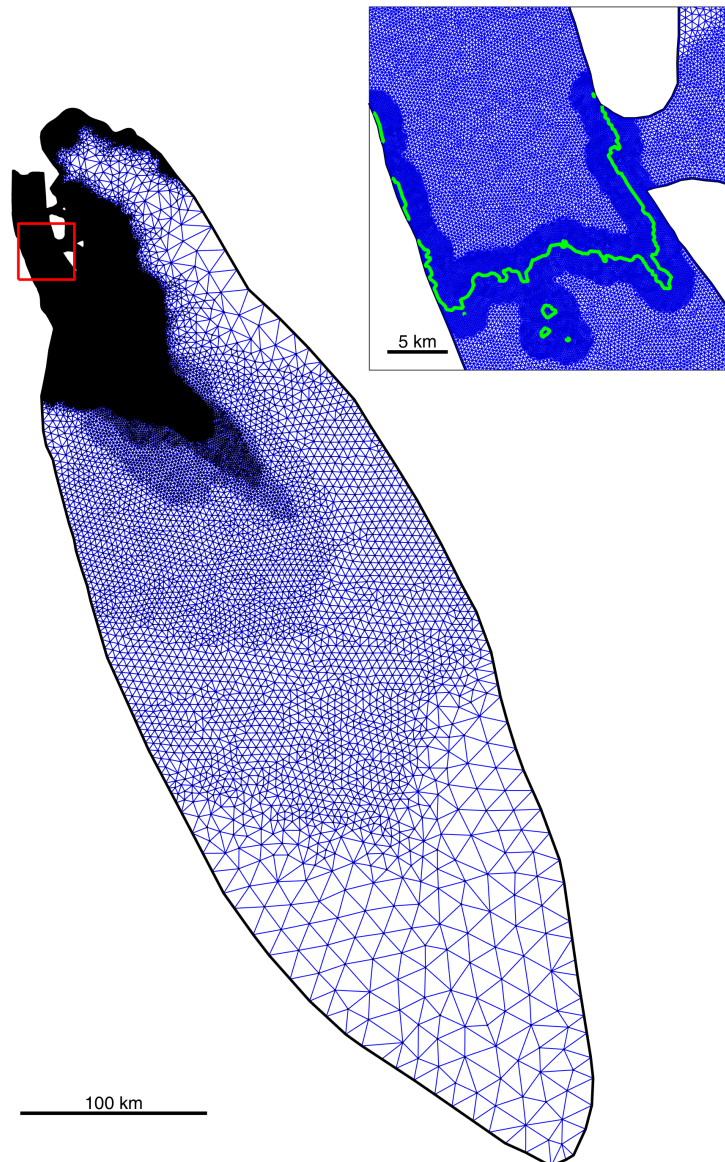


Fig. 1. Initial finite linear-element mesh across the Petermann Glacier catchment (black line) which acts as our model domain. This mesh has 111391 elements, and 56340 nodes, and is refined in areas of low elevation, along the floating ice tongue, and where the ice is flowing fastest. Inset shows the mesh refinement along the ice tongue (300 m element size) and around the grounding line (100 m element size) (green line)

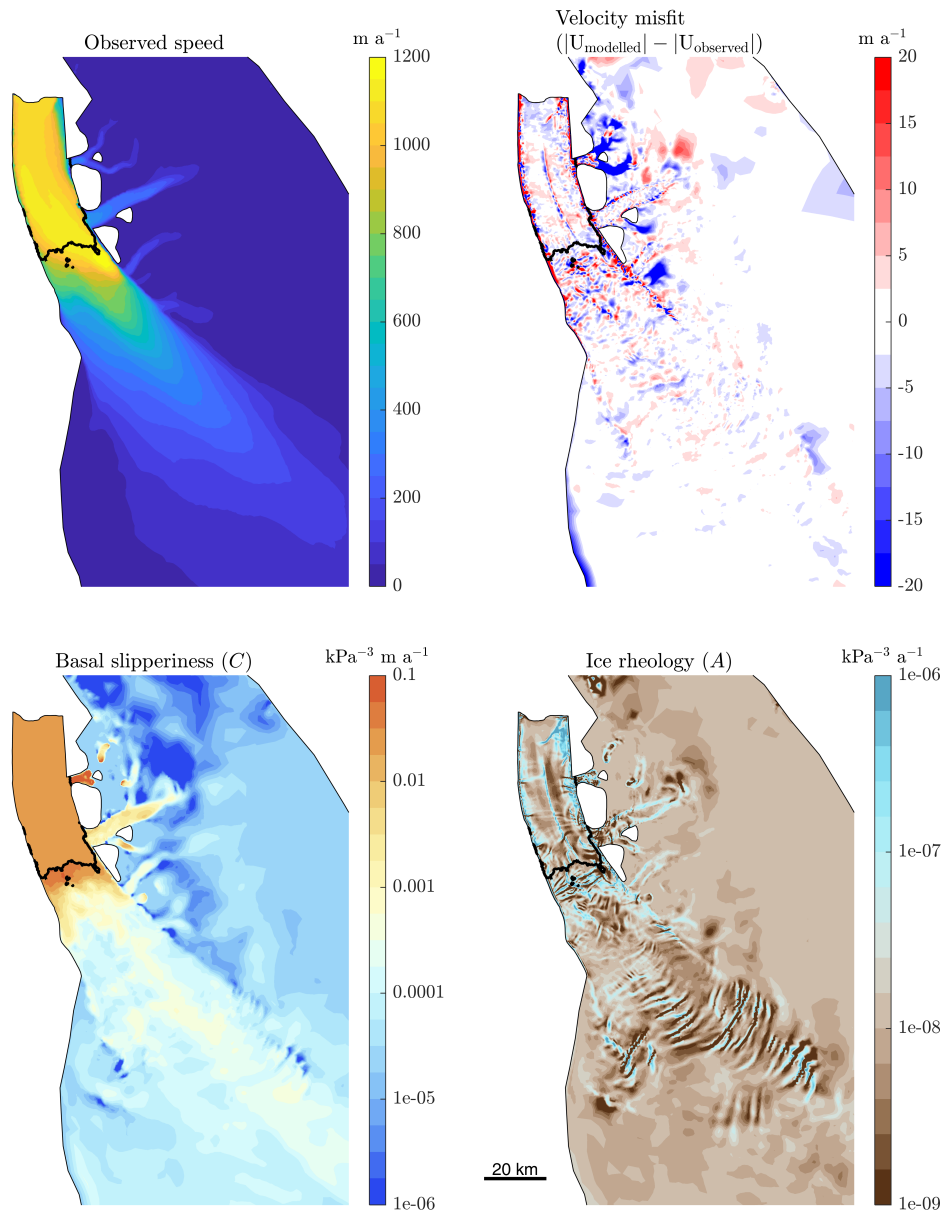


Fig. 2. Results from model inversion. Top left panel shows observed ice flow speeds, where flow speeds reach up to 1200 m a^{-1} along the ice tongue. Top right panel shows the misfit between observed and modeled ice flow speeds after inversion. The bottom left panel shows basal slipperiness (C) using $m=3$. Light blue through to light and dark orange show areas of slipperiest ice. Note the slippery bed within $\sim 10 \text{ km}$ inland of the grounding line. We also set slipperiness values below the ice tongue to be the same as the average C value within 10 km inland of the grounding line to prevent advance into unrealistically stiff bed conditions. Bottom right panel shows ice rheology parameter (A) from Glen's flow law using $n=3$. Areas of light to dark turquoise represent the softest ice, while dark brown is the areas of stiffest ice. Note the areas of weak ice in the downstream section of the ice shelf and along the lateral margins.

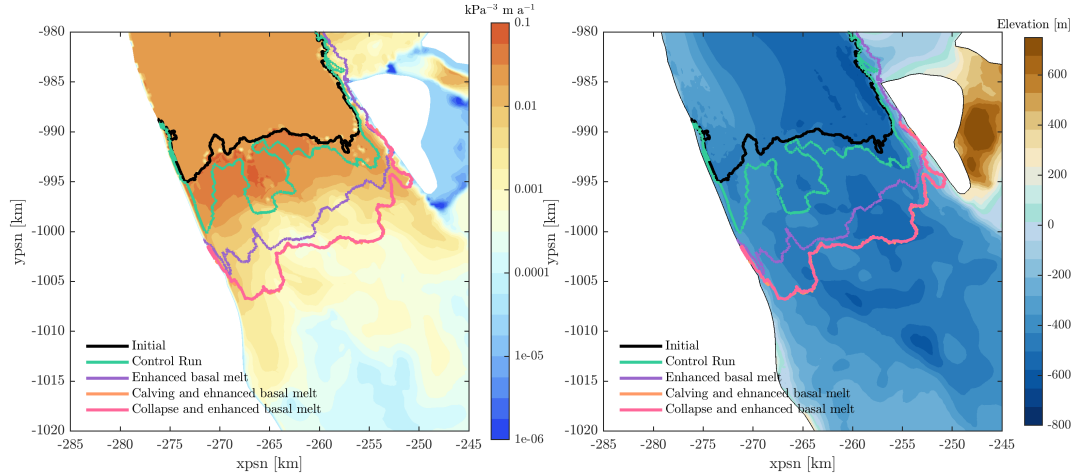


Fig. 3. Left panel shows the basal slipperiness from our inversion (C), where orange represents high basal slipperiness, and blue is low basal slipperiness. The right panel shows the bed topography from the Operation IceBridge BedMachine v3 dataset (Morlighem and others, 2017), where blue is elevation below sea level and green-brown is above sea level. The initial grounding line position at time=0 is shown in black. Grounding line positions after 100 years for each model run are: control run (green), enhanced basal melt (purple), calving and enhanced basal melt (orange) and ice shelf collapse and enhanced basal melt (pink).

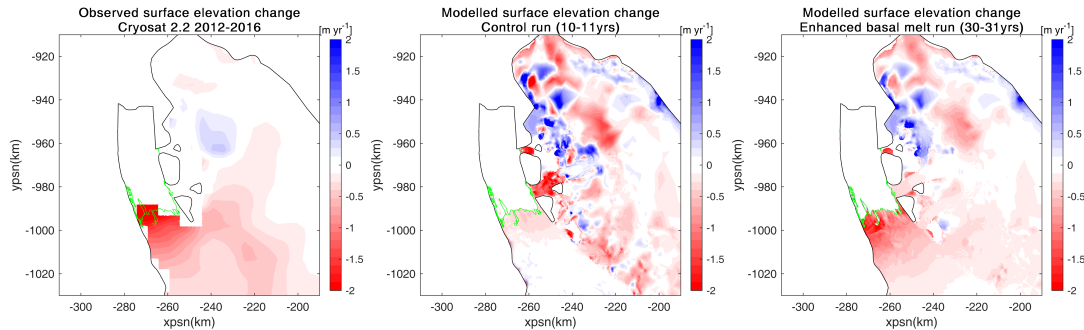


Fig. 4. Observed and modelled rates of elevation change. Left plot is observed surface elevation change from the Cryosat 2.2 satellite averaged between 2012-2016, which is similar to the date range of our input SMB from RACMO (2011-2016). Middle plot shows modelled surface elevation change at the beginning of our control run (10-11 yrs). As expected, due to prescribing lower basal melt rates than observed during 2012-2016 (Wilson and others, 2017), our elevation changes underestimate observations. As way of comparison, the right hand plot shows surface lowering during our enhanced basal melt rates (at the point at which the glacier begins to respond dynamically to higher melt rates: 30yrs), which show a better fit to observed elevation changes.

S1. SENSITIVITY TO MESH RESOLUTION

Initially we use a linear element mesh with 111391 elements and 56340 nodes (Figure 1). As discussed in the main body of the text this mesh was refined by three criteria: floating ice, flow speeds, surface elevation. Along the ice tongue, where flow is fastest and at low elevations element sizes were set to 300 m. We then refine the mesh around the grounding line at each time-step. Within 2 km of the grounding line element sizes were set to 100 m. To test the robustness of our results with respect to mesh resolution around the grounding line, we repeat our control run with a series of different element sizes around the grounding line. We do this for 50 m, 100 m (our initial element size), 150 m, 200 m, 250 m and 300 m. As element sizes were refined to 300 m across the ice tongue any further increases in grounding line element size (>300) would no longer be refining elements around the grounding line. Figure 5 shows the change in ice volume above flotation (VAF) in Gt between time=0 and time=100 for each mesh size refinement. This shows that there is little variability between ice volume loss based on the refinement of the mesh size around the grounding line. VAF for all mesh size experiments were within the range of ± 2.2 Gt, which is only 1.3% of the mean ice loss for all experiments (-155.7 Gt). This demonstrates that our transient experiments were insensitive to the size of the grounding line mesh refinement.

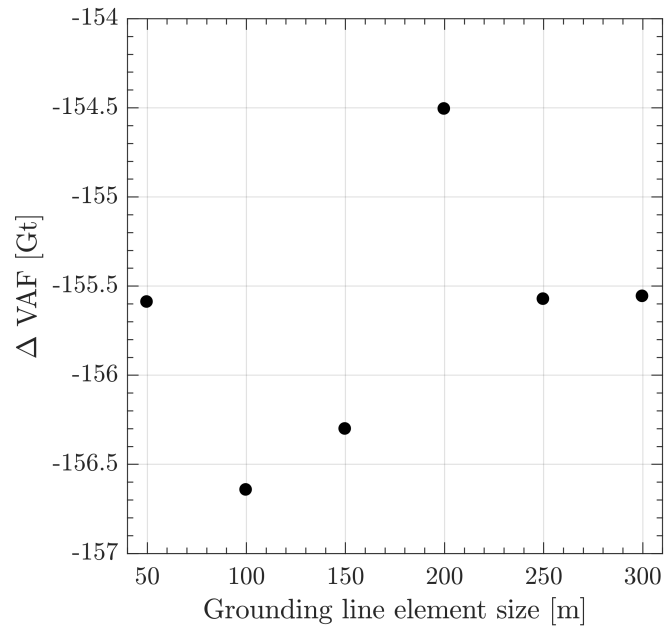


Fig. 5. Change in ice volume above flotation (VAF) over 100 yrs in Gt for control runs executed using different sized elements within 2 km of the grounding line.

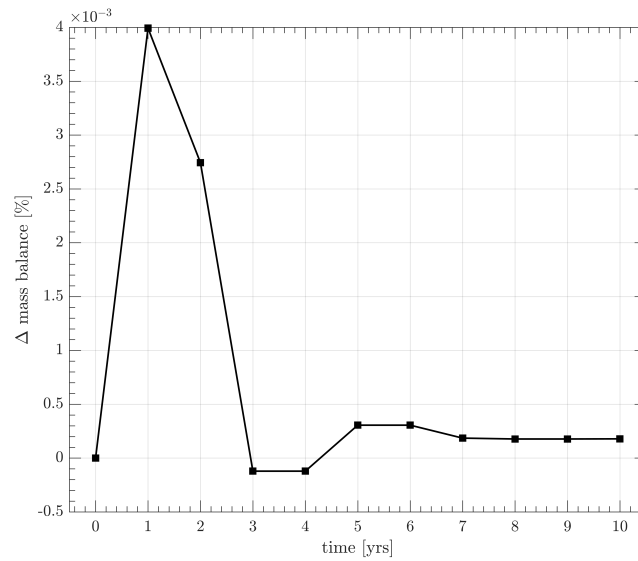


Fig. 6. Percentage change (10^{-3} %) in total mass balance relative to initial conditions (time=0) during the model relaxation period of 10-years.

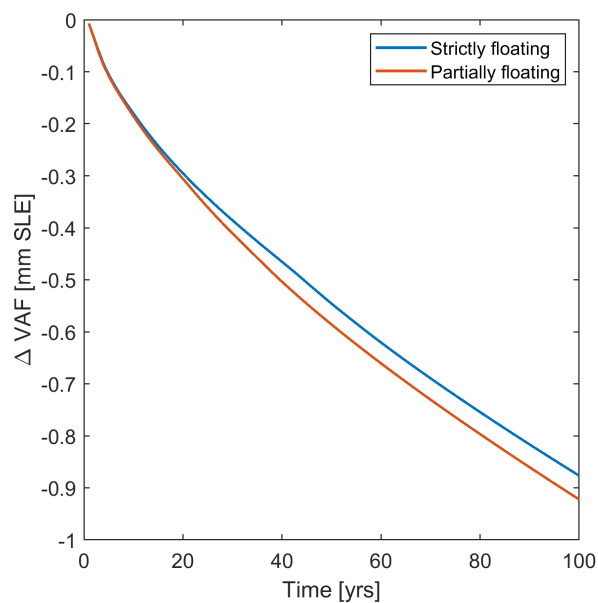


Fig. 7. Sensitivity of our results to melting in fully floating nodes and partially floating nodes for our third experiment in which we immediately remove the ice shelf and apply enhanced basal melting to newly floating nodes.

REFERENCES

- Morlighem M, Williams CN, Rignot E, An L, Arndt JE, Bamber JL, Catania G, Chauché N, Dowdeswell JA, Dorschel B, Fenty I, Hogan K, Howat I, Hubbard A, Jakobsson M, Jordan TM, Kjeldsen KK, Millan R, Mayer L, Mouginot J, Noël BP, O’Cofaigh C, Palmer S, Rysgaard S, Seroussi H, Siegert MJ, Slabon P, Straneo F, van den Broeke MR, Weinrebe W, Wood M and Zinglensen KB (2017) BedMachine v3: Complete Bed Topography and Ocean Bathymetry Mapping of Greenland From Multibeam Echo Sounding Combined With Mass Conservation. *Geophysical Research Letters*, **44**(21), 051–11, ISSN 19448007 (doi: 10.1002/2017GL074954)
- Wilson N, Straneo F and Heimbach P (2017) Satellite-derived submarine melt rates and mass balance (2011-2015) for Greenland’s largest remaining ice tongues. *Cryosphere*, **11**(6), 2773–2782, ISSN 19940424 (doi: 10.5194/tc-11-2773-2017)